

## Simulation of solar energetic particle events with a data-driven physics-based transport model

---

Ming Zhang<sup>a,\*</sup> and Lei Cheng<sup>a</sup>

<sup>a</sup>*Department of Aerospace, Physics and Space Sciences, Florida Institute of Technology  
150 W. University Blvd, Melbourne, FL 32940, USA*

*E-mail:* [mzhang@fit.edu](mailto:mzhang@fit.edu)

Solar energetic particles (SEPs) are accelerated by CMEs or solar flares. They travel through the corona and interplanetary magnetic fields to reach Earth, becoming a radiation hazard dangerous to astronauts working in space and electronics on spacecraft. Because each event has unique magnetic field properties and solar eruption kinematics, a data-driven model is necessary to predict SEP hazards. We have developed a model using photospheric magnetic field measurements and observed CME shock as inputs. The model incorporates diffusive shock acceleration with an injection of source particles from heated solar wind ions by CME shock. Testing its performance with simulation of several historical SEP events yields good agreement with observed time-intensity profiles and spectrum, particularly for weak CMEs or on magnetic field lines not connected to a strong shock. The model requires appropriate input of particle diffusion coefficient in order to reproduce the particle time-intensity profiles, but the peak intensity is less critically dependent on the diffusion coefficient.

38th International Cosmic Ray Conference (ICRC2023)  
26 July - 3 August, 2023  
Nagoya, Japan



---

\*Speaker

## 1. Introduction

Solar energetic particles (SEPs) are accelerated by shock waves driven by coronal mass ejections (CMEs) and in the processes of magnetic reconnection associated with solar flares. The high-energy (> 30 MeV) SEP components are of great concern as a space weather hazard because they are hard to shield and can do severe damage to human and electronics in space. These particles are produced deep in the solar corona or near the solar surface where solar flares take place, CME shocks are thought to be more efficient in particle acceleration, and seed particle populations injected into the processes of particle acceleration are more abundant.

Radiation intensity at any location in interplanetary space depends on how SEPs propagate through the coronal and heliospheric magnetic fields. Sometimes, SEPs can come from seemingly unconnected solar flares or CMEs, probably due to particle transport across the average magnetic field lines through field line random walk occurring on the micro-scales that we cannot observe or model easily. This makes it particularly hard to predict SEP events. Also, the large-scale field geometry of the corona is quite complex, and it can vary tremendously from event to event. So, the best predictive tools must use remote observations of solar flares and CME shocks as well as solar, coronal, and heliospheric magnetic fields based on measurements such as photospheric magnetograms. These observations in real-time are reliable information about the SEP source-producing region and the magnetic medium where SEPs propagate, thus giving us lead time to prepare for radiation hazards.

We have built a physics-based model of solar energetic particle source and transport using a combination of observation-based products, including coronal magnetic field models extrapolated from photospheric field measurements and the characteristics of solar flares or CME shocks reconstructed from coronagraph observations. The basic methodology of our model consists of solving the focused transport equation of SEP propagation that includes essentially all physical transport mechanisms: particle streaming, convection, gradient/curvature drift, adiabatic cooling, magnetic focus, pitch-angle scattering, and perpendicular diffusion. It is solved using a Monte Carlo technique based on the corresponding stochastic differential equations for tracing random trajectories of particle guiding centers using time-backward approaches. Because we rigorously solve the diffusion equation, the model is especially good at predicting poorly connected events. This paper shows case studies and simulation results successfully used to explain observed features of SEP events.

## 2. Model

The equation governing the particle distribution function  $f(t, \mathbf{r}, p, \mu)$  as a function of time  $t$ , position  $\mathbf{r}$ , momentum magnitude  $p$  and pitch-angle cosine  $\mu$  is written as [15, 16]:

$$\frac{\partial f}{\partial t} = \nabla \cdot \boldsymbol{\kappa}_{\perp} \cdot \nabla f - (v\mu\hat{\mathbf{b}} + \mathbf{V} + \mathbf{V}_d) \cdot \nabla f + \frac{\partial}{\partial \mu} D_{\mu\mu} \frac{\partial f}{\partial \mu} - \frac{d\mu}{dt} \frac{\partial f}{\partial \mu} - \frac{dp}{dt} \frac{\partial f}{\partial p} + Q. \quad (1)$$

where  $Q$  is the particle source injection rate. It includes perpendicular diffusion with a tensor  $\boldsymbol{\kappa}_{\perp}$ , pitch angle diffusion with a coefficient  $D_{\mu\mu}$ , streaming along the magnetic field direction  $\hat{\mathbf{b}}$  with particle speed  $v$ , convection with the solar wind plasma  $\mathbf{V}$ , particle gradient/curvature drift

$\mathbf{V}_d$ , focusing  $\frac{d\mu}{dt}$  and adiabatic cooling  $\frac{dp}{dt}$  in a nonuniform plasma and magnetic field. The drift velocity, focusing, and adiabatic cooling can be determined through magnetic field  $\mathbf{B}$  and plasma velocity  $\mathbf{V}$  based on adiabatic approximation valid under the condition of small gyroradius and fast gyration compared the gradients and time variation of all the variables in Equation (1):

$$\mathbf{V}_d = \frac{cpv}{qB} \left\{ \frac{1-\mu^2}{2} \frac{\mathbf{B} \times \nabla B}{B^2} + \mu^2 \frac{\mathbf{B} \times [(\mathbf{B} \cdot \nabla)\mathbf{B}]}{B^3} + \frac{1-\mu^2}{2} \frac{\mathbf{B}(\mathbf{B} \cdot \nabla \times \mathbf{B})}{B^3} \right\} \quad (2)$$

$$\frac{d\mu}{dt} = -\frac{(1-\mu^2)v}{2} \hat{\mathbf{b}} \cdot \nabla \ln B + \frac{\mu(1-\mu^2)}{2} (\nabla \cdot \mathbf{V} - 3\hat{\mathbf{b}}\hat{\mathbf{b}} : \nabla \mathbf{V}) - \frac{(1-\mu^2)p}{v} (\mathbf{V} \cdot \nabla \mathbf{V}) \cdot \hat{\mathbf{b}} \quad (3)$$

$$\frac{dp}{dt} = -\left[ \frac{1-\mu^2}{2} (\nabla \cdot \mathbf{V} - \hat{\mathbf{b}}\hat{\mathbf{b}} : \nabla \mathbf{V}) + \mu^2 \hat{\mathbf{b}}\hat{\mathbf{b}} : \nabla \mathbf{V} \right] p - \frac{\mu p}{v} (\mathbf{V} \cdot \nabla \mathbf{V}) \cdot \hat{\mathbf{b}} \quad (4)$$

The second-order partial derivative terms in Equation (1), i.e., spatial perpendicular diffusion and pitch angle diffusion, represent the effects of magnetic field turbulence on particle transport. We neglected other components of particle diffusive transport in momentum because heliospheric magnetic turbulence is typically Alfvénic, so the rate of momentum fluctuation is only  $V_A/v \ll 1$  ratio times that of pitch angle scattering. In addition, we have neglected cross diffusion term like  $D_{\perp\mu}$  because diffusion in  $\mu$  is typically driven by field fluctuation resonating with particle gyration, while diffusion in perpendicular spatial coordinates is driven by field line random walk in the heliospheric plasmas.

We solve the focus transport equation (1) through time-backward Monte-Carlo simulation based on stochastic differential equations that give rise to the diffusion equation. See [14] or [15, 16] for details on solving diffusion equations with initial/boundary value or source term using stochastic simulation.

Equation (1) requires an input of  $\mathbf{V}$  and  $\mathbf{B}$  everywhere in the simulation domain. In our data-driven approach to the prediction of actual events, we rely on magnetogram measurements of the photosphere. Fields everywhere else in the solar corona and heliosphere are extrapolated from the photosphere using a model. Three types of magnetic field model have been implemented:

- Potential Field Source Surface (PFSS) [1, 12]
- Horizontal Current-Current Sheet-Source Surface (HCCSSS) [18, 19]
- CorHel MHD solar magnetic field model by Predictive Science Inc. [5, 8–11].

The PFSS and HCCSSS models do not have plasma properties. We use an empirical solar wind model proposed by Leblanc et al. [7], which prescribes the radial solar wind speed  $V_r$  and density  $n$  as functions of radial distance. The terminal velocity of solar wind and density at 1 AU are adjustable parameters to match observation at 1 AU at the time of the solar event.

A CME shock is inserted into the magnetic field and plasma model. We take a data-driven ellipsoid model of CME shock from Kwon et al. [6], who developed a robust technique that allows us to determine from multipoint (STEREO, SOHO, and SDO) coronagraph observations the extent, shape, kinematics, and density compression ratios of coronal shocks. The shocks can be identified with sharp but faint brightness enhancements seen ahead of and around bright CME fronts in coronagraph images. Using the input of plasma information from the plasma and magnetic field models, we can determine the shock parameters everywhere on the surface, such as shock speed

$V_{sh}$ , fast magnetosonic (nearly Alfvénic) Mach number  $M$ , and shock obliquity  $\theta_{bn}$ . These numbers are further used to determine the shock compression ratio  $R$  everywhere on the surface using the shock adiabatic equation [e.g., 2, 13]. The shock compression ratio is crucial for the input of SEP source.

A typical CME shock can only be observed in the corona up to ten solar radii or so, either because of going out of the field of instrument view or becoming too dim. We use a CME propagation model suggested by Corona-Romero et al. [4] to extrapolate its propagation further into the interplanetary medium. The model can capture the slowdown of CME and its shock so that we do not overestimate particle acceleration in interplanetary space.

We inject accelerated SEP particles at the shock. According to the theory of diffusive shock acceleration, the spectrum of acceleration particles is a known power law  $\propto p^{-\gamma_s}$  with a spectral slope  $\gamma_s = 3R/(R - 1)$ . We just need the total of seed particles injected to determine the level of particle intensity. Such power-law distribution is valid up a cutoff momentum  $p_c$  which is only determined by the local shock condition and age through:

$$t = \bar{t}(p_c) = \int_{p_{inj}}^{p_c} \frac{3}{V_{n1} - V_{n2}} \left[ \frac{\kappa_1(p')}{V_{n1}} + \frac{\kappa_2(p')}{V_{n2}} \right] \frac{dp'}{p'} \quad (5)$$

where  $t$  is shock age since initiation,  $\bar{t}(p_c)$  is the time needed to accelerate the particle from injection momentum  $p_{inj}$  to  $p_c$ .  $V_{n1,2}$  and  $\kappa_{1,2}$  are plasma velocity and particle diffusion coefficient, upstream (denoted by 1) and downstream (denoted by 2) of the shock. Typically only upstream conditions are important in determining the cutoff momentum. We choose the Bohm diffusion limit for  $\kappa_1$ , which could somewhat overestimate the cutoff momentum.

We inset a SEP source at the shock  $\mathbf{r}_{sh}$  with a rate

$$Q(p) = -N \left( \frac{p}{p_{inj}} \right)^{-\gamma_s} \delta(\mathbf{r} - \mathbf{r}_{sh}) \quad \text{for } p < p_c \quad (6)$$

The input of  $N$  requires details of particle injection into diffusive shock acceleration. We assume that the seed particles are mainly suprathermal solar wind ions heated by the CME shock. A simple way for determining the level of SEP source injection level is to pick a characteristic injection velocity  $v_{inj}$ . Then  $N$  is given as the value of Maxwellian distribution, i.e.,

$$N = \eta(\theta_{bn}) \frac{n_{sw2} V_{n1}}{(4\pi v_{th2}^2)^{3/2}} \exp\left(-\frac{v_{inj}^2}{v_{th2}^2}\right) \quad (7)$$

with an obliquity-dependent injection efficiency  $\eta(\theta_{bn})$ . We use  $\eta(\theta_{bn}) = 0.08 - 0.07 \tanh[(\theta_{bn} - 60^\circ)/10^\circ]$  from Caprioli & Spitkovsky [3].  $n_{sw2}$  and  $v_{th2}$  are the downstream solar wind density and thermal speed. They can determine from their corresponding upstream values with the help of the shock compression ratio.  $v_{inj}$  is a free parameter that controls the level of SEP intensity. Typically, a  $v_{inj}$  between  $2.3 - 2.7 V_{n1}$  can produce a good fit to observations.

The model requires inputs of diffusion coefficients,  $D_{\mu\mu}$  and  $\kappa_{\perp}$ . We use quasilinear theory for the pitch angle diffusion driven by a Kolmogorov Alfvénic turbulence,

$$D_{\mu\mu} = D_0(\mathbf{x}) p^{q-2} (1 - \mu^2) (|\mu|^{q-1} + h_0) \quad (8)$$

with  $q = 5/3$  and  $h_0 = 0.2$  for minimum resonant gap.  $D_0$  is a free parameter that can be used to quantify the particle mean free path. For the perpendicular diffusion, we use Zhang and Zhao [17]

$$\kappa_{\perp} = \frac{v}{2V} \alpha_{\perp} \kappa_{gd0} \frac{B_0}{B} \quad (9)$$

where  $\alpha$  is a free tuning parameter to dial down the diffusion rate from the photospheric diffusion rate  $\kappa_{gd0} = 3.4 \times 10^{13} \text{ cm}^2\text{s}^{-1}$  estimated from a typical speed of supergranular motion.  $v/V$  is the ratio of particle to solar wind plasma speed, and  $B/B_0$  is the ratio of the magnetic field relative to its value on the solar surface  $B_0$  on the same field line.

### 3. Results

We have simulated several SEP events, all of which have well-observed CME shocks in coronagraph measurements so that we can reconstruct a series of ellipsoid shock surfaces. Here we concentrate on the comparison of predicted time-intensity profiles with observations for a selected number of events.

#### 3.1 2011 November 3 event

We have made simulations of this event as observed by spacecraft at Earth, STEREO-A (STA), and STEREO-B (STB) locations. One of the calculations shown in Figure 1 is based on the MHD solution of the corona and heliosphere obtained by Predictive Science Inc, and the other in Figure 2 is based on the PFSS model with the input of spherical harmonic coefficients published by Global Oscillation Network Group at the National Solar Observatory. The time-intensity profiles at Earth and STB fit observation observations quite well for several low-energy channels, but they become inconsistent for high-energy channels above 40 MeV, indicating there might be a problem in the estimation of shock cutoff energy. The particles in the low-energy channels are below the shock acceleration cutoff energies in the corona. The High-energy channels are above the shock cutoff. The simulations at STA can reproduce the time-intensity profiles in energy channels below the calculated energies. Zhang et al. [16] pointed out that this is an effect of shock-generated turbulence that change the diffusion coefficient on the magnetic field lines connected to STA.

#### 3.2 2013 April 11 event

Figure 3 shows simulation results for Earth and STB based on the PFSS coronal magnetic field model. They produce an excellent fit to the observed SEP time-intensity profiles in nearly every energy channel. The highest energy, 80 MeV channel at Earth, over-predicts the observation, probably due to a slight overestimation of shock cutoff at its particle source locations. The lowest 2 MeV channel at STB slightly over-predicts, perhaps because these particles are affected by shock-generated turbulence on the field lines leading to STB with higher levels of SEP intensity.

#### 3.3 2011 March 7 event

Figure 4 shows the result of simulations for spacecraft at Earth, STB, and STA based on the PFSS coronal magnetic field model. The time-intensity profiles at Earth and STB match observations quite well, except for the highest 80 MeV energy channel due to an overestimation

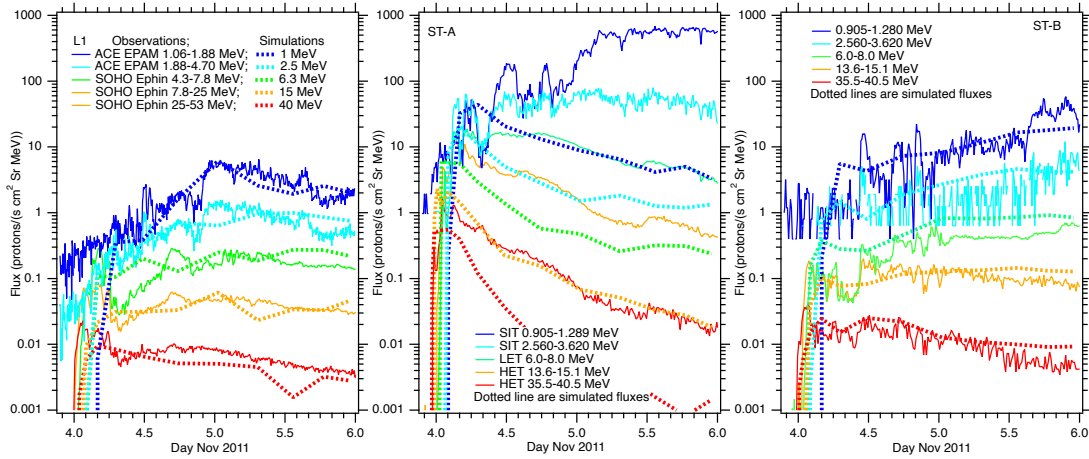


**Figure 1:** Proton fluxes at selected energy levels and comparison with observations by *SOHO/ACE* at Earth, STA, and STB during the 2011 Nov 3 SEP event. The dotted traces are simulation results calculated with an MHD model of the corona and heliosphere. (From [16])

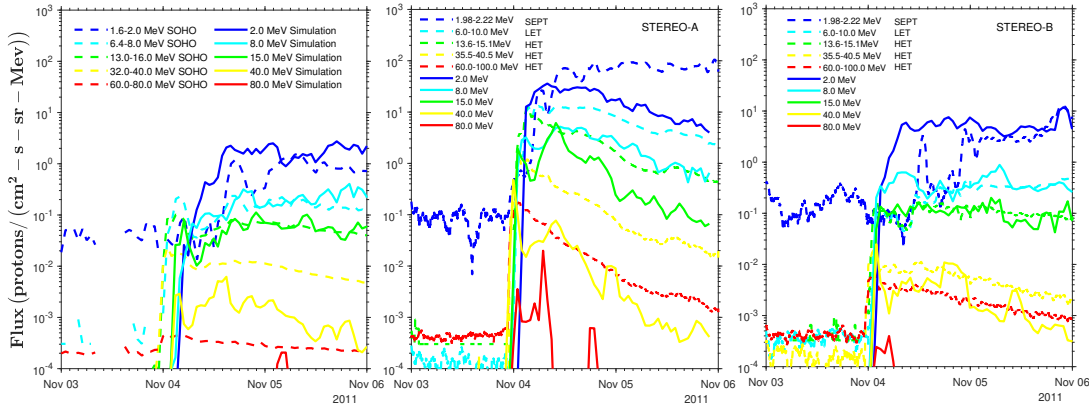


**Figure 2:** Proton fluxes at selected energy levels and comparison with observations by *SOHO/ACE* at Earth, STA and STB during the 2011 Nov 3 SEP event. The solid traces are simulation results calculated with a PFSS model of the coronal magnetic field and LeBlanc (1998) empirical solar wind model.

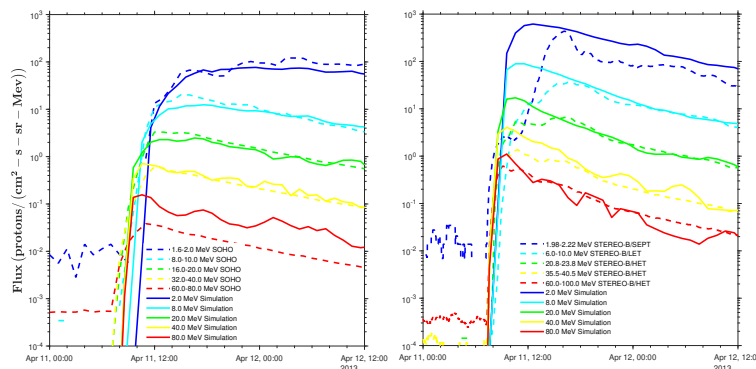


**Figure 3:** Proton fluxes at selected energy levels and comparison with observations by *SOHO* at Earth and STB during the 2013 April 11 SEP event. The solid traces are simulation results calculated with a PFSS model of the coronal magnetic field and LeBlanc (1998) empirical solar wind model.

POS (ICRC2023) 1275

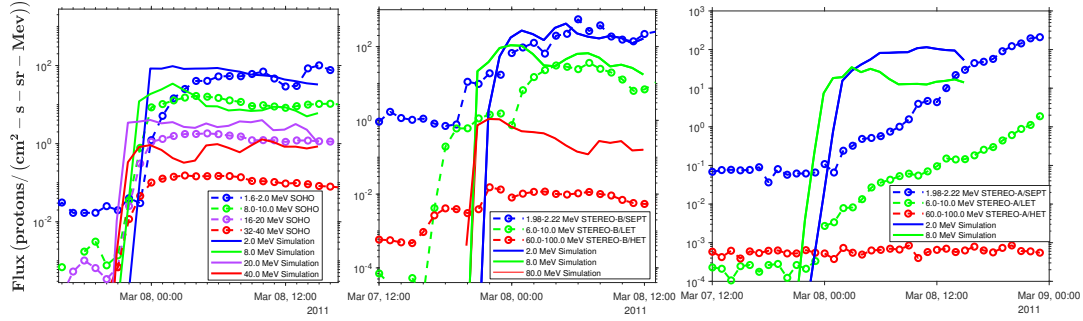


**Figure 4:** Proton fluxes at selected energy levels and comparison with observations by *SOHO* at Earth and STB during the 2011 March 7 SEP event. The solid traces are simulation results calculated with the PFSS model of coronal magnetic field and LeBlanc (1998) empirical solar wind model.

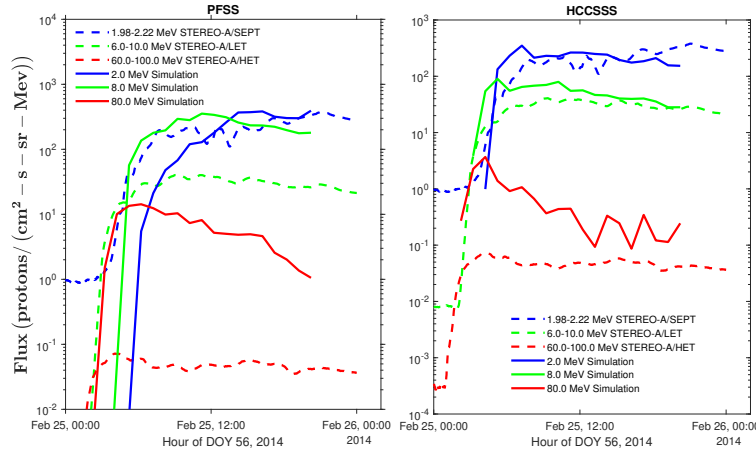


**Figure 5:** Proton fluxes at selected energy levels and comparison with observations by *SOHO* at STA during the 2014 February 25 SEP event. The solid traces are simulation results calculated with a PFSS model (left) and HCCSSS model (right) of the coronal magnetic field and both with LeBlanc (1998) empirical solar wind model.

of shock cutoff energy. The time-intensity profiles predicted for STA rise much faster than the observations. STA sat on magnetic field lines connected to the edge of the CME shock. The simulation result is sensitive to the magnetic connectivity in this case. In our simulation, STA is well connected to the CME shock at the beginning of the event, but the observations suggest otherwise. Simulation with different magnetic field models might resolve this issue.

### 3.4 2014 February 25 event

Figure 5 shows the simulations for STA with two different coronal magnetic field models: (left) the PFSS model and (right) the HCCSSS model. With the PFSS model, the predicted time-intensity profiles can only match one of the channels. However, with the HCCSSS magnetic field model, fits to observations are improved in all energy channels. The over-prediction in the highest 80 MeV energy channel is improved, but it still needs adjustment for the estimate of shock cutoff.

#### 4. Summary

We have developed a data-driven model to predict SEP intensity accelerated by CME shocks. The model can take several forms of magnetic field and plasma distribution for the solar corona and heliosphere. With the input of observationally reconstructed CME shock and its propagation, the model can predict absolute SEP intensity without normalizing to observations. Tests with case studies based on several past SEP events show quite good performance compared to observations. The match appears particularly well at low energies below the shock acceleration cutoff energy. When the particle intensity is high enough, the model needs improvement in treating wave-particle interactions that can affect the propagation of low-energy SEPs escaping from the shock. The model with a Bohm diffusion limit tends to estimate shock acceleration cutoff, thus over-predicting the particle intensity at high energies near the shock cutoff.

#### References

- [1] Altschuler, M. D. & Newkirk, G. 1969, *Solar Phys.*, 9, 131.
- [2] Kabin, K., 2001, *J. Plas. Phys.*, 66, 259-274
- [3] Caprioli, D. & Spitkovsky, A. 2014, *Astrophys. J.*, 783, 91
- [4] Corona-Romero, P., et al., 2013, *Solar Phys.*, 285, 391-410.
- [5] Downs, C., Lionello, R., Mikić, Z., et al. 2016, *Astrophys. J.*, 832, 180.
- [6] Kwon, R.-Y., Zhang, J., & Olmedo, O. 2014, *Astrophys. J.*, 794, 148.
- [7] Leblanc, Y., Dulk, G. A., & Bougeret, J.-L. 1998, *Solar Phys.*, 183, 165.
- [8] Lionello, R., Linker, J. A., & Mikić, Z. 2001, *Astrophys. J.*, 546, 542.
- [9] Mikic, Z. & Linker, J. A. 1994, *Astrophys. J.*, 430, 898.
- [10] Riley, P., Linker, J. A., & Mikić, Z. 2001, *J. Geophys. Res.*, 106, 15889.
- [11] Riley, P., Lionello, R., Linker, J. A., et al. 2011, *Solar Phys.*, 274, 361.
- [12] Schatten, K. H., Wilcox, J. M., & Ness, N. F. 1969, *Solar Phys.*, 6, 442.
- [13] Thompson, W. B., 1962, *An Introduction to Plasma Physics*, Addison Wesley
- [14] Zhang, M. 1999, *Astrophys. J.*, 513, 409.
- [15] Zhang, M., Qin, G., & Rassoul, H. 2009, *Astrophys. J.*, 692, 109.
- [16] Zhang, M., Cheng, L., Zhang, J., et al. 2023, *Astrophys. J. Supp.*, 266, 35.
- [17] Zhang, Ming and Zhao, Lulu, 2017, *Astrophys. J.*, 846, 107.
- [18] Zhao, X. & Hoeksema, J. T. 1994, *Solar Phys.*, 151, 91.
- [19] Zhao, X. & Hoeksema, J. T. 1995, *J. Geophys. Res.*, 100, 19.